Summary: Nanofibrous non-woven matrices were prepared by electrospinning a regenerated silk fibroin (SF) solution, and the structural changes of SF nanofibers treated with water vapor were investigated using time-resolved IR and ^{13}C CP/MAS NMR spectroscopy. Conformational transitions of SF from random coil to β-sheet structures were induced by water vapor treatment and were strongly dependent on the treatment time and temperature. Water vapor treatment provided a useful means of stabilizing the SF nanofiber matrices, resulting in the formation of matrices with a decreased solubility in water and increased mechanical strength. The adhesion and spreading of both normal human keratinocytes and fibroblasts onto the SF nanofiber matrices were also investigated, and the water vapor-treated SF nanofiber matrices showed good cellular compatibility, in comparison with traditional methanol-treated ones. This approach to controlling the conformational changes of SF nanofibers by water vapor treatment may be useful in the design and tailoring of novel materials for biomedical applications, including wound dressings and scaffolds for tissue engineering.

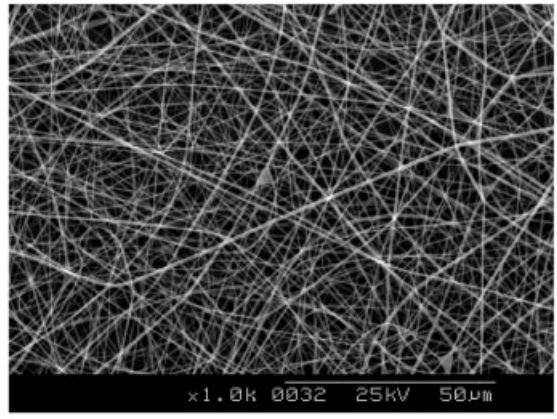

Scanning electron microscopic pictures of water vapor-treated SF nanofibers.

Regenerated Silk Fibroin Nanofibers: Water Vapor-Induced Structural Changes and Their Effects on the Behavior of Normal Human Cells

Byung-Moo Min,[1] *Lim Jeong,*[2] *Kuen Yong Lee,**[3] *Won Ho Park**[2]

[1] Department of Oral Biochemistry and Craniomaxillofacial Reconstructive Science, Dental Research Institute, and BK21 HLS, Seoul National University College of Dentistry, Seoul 110-749, South Korea
[2] Department of Textile Engineering, College of Engineering, Chungnam National University, Daejeon 305-764, South Korea
Fax: +82-42-823-3736; E-mail: parkwh@cnu.ac.kr
[3] Department of Bioengineering, College of Engineering, Hanyang University, Seoul 133-791, South Korea
Fax: +82-2-2293 2642; E-mail: leeky@hanyang.ac.kr

Received: December 22, 2005; Revised: February 14, 2006; Accepted: February 14, 2006; DOI: 10.1002/mabi.200500246

Keywords: β-sheet conformation; cell behavior; nanofiber; silk fibroin; structural changes

Introduction

Fibroin is a main component of silkworm silk, and is responsible for the unique physical and chemical characteristics of silk.[1] Silk fibroin (SF) can be prepared in various forms, such as gels, powders, fibers, and membranes.[2–6] SF has been widely used for cosmetics and food additives,[7,8] and has recently found potential applications in the areas of biomedical science and engineering[9,10] due to its distinctive biological properties. SF has attracted much attention to date due to its biocompatibility, oxygen and water vapor permeability, biodegradability, and minimal inflammatory reactions.[11–13] One of the promising applications of SF in biomedical engineering is as a scaffolding material for tissue engineering. It was reported that SF matrices could be useful in the culture of fibroblasts and osteoblasts, as well as stem cells, and could enhance the adhesion, growth, and differentiation of the cells in a manner similar to that of collagen matrices.[14–17]

We have previously reported that nonwoven matrices of electrospun nanofibers can be prepared from a regenerated SF solution, and that the matrices were effective in cell

attachment and spreading of normal human keratinocytes and fibroblasts.[18,19] However, electrospun SF nanofibers, as well as other types of SF matrices such as films, should be typically followed by chemical treatment with an aqueous alcohol solution in order to increase their stability and mechanical properties in the presence of water.[20,21] Methanol has been frequently used for this purpose, and SF matrices that are not treated with an aqueous methanol solution can easily dissolve or swell in water. Thus, the solvent-induced structural changes of SF have been widely investigated and utilized to form stable SF matrices.[20,21] However, methanol-treated SF matrices are often brittle due to their high content of crystalline regions. It was reported that a water-based annealing procedure also provided a useful method of preparing water-stable SF matrices.[22,23] However, this approach was only effective for matrices of a certain thickness. In this paper, we report a novel approach to stabilizing electrospun SF nanofibers by treatment with water vapor instead of alcohol solutions. The solvent-induced conformational changes of SF treated with water vapor was investigated and compared with methanol-treated SF nanofiber matrices. The structural changes of SF nanofibers were studied using IR and NMR spectroscopy. A custom-made chamber was used for measurements of time-resolved infrared spectra of the SF nanofibers during the water vapor treatment. The effect of the water vapor treatment on the adhesion and spreading of normal human keratinocytes and fibroblasts was also investigated *in vitro*.

Experimental Part

Regenerated Silk Fibroin Solution

Degummed silk yarn was dissolved in a ternary solvent system composed of calcium chloride, ethanol, and water (1:2:8 molar ratio) at 70 °C for 6 h, followed by dialysis with cellulose tubular membranes (molecular weight cut-off, 12 000; Sigma) against distilled water for 3 d. The resultant solution was filtered and lyophilized to obtain a white powder. The SF powder was then dissolved in 1,1,1,3,3,3-hexafluoro-2-propanol (HFIP) to prepare a regenerated SF solution.

Electrospun Silk Fibroin Nanofibers

The SF nanofibers were prepared by electrospinning a 7% (w/v) regenerated silk fibroin solution, and were collected on a target drum that was placed at a distance of 8 cm from the syringe tip (inner diameter 0.0838 mm). A voltage of 16 kV was applied to the collecting target by a high voltage power supply, and the flow rate of the solution was 2 $mL \cdot min^{-1}$.

Treatment of Electrospun Silk Fibroin Nanofibers

Electrospun SF nanofiber matrices were either treated with an aqueous methanol solution or exposed to an atmosphere of water vapor to achieve the solvent-induced crystallization of fibroin. Briefly, the nanofiber matrices were treated with an aqueous methanol solution (50%), rinsed with distilled water, and dried in a vacuum at room temperature for 24 h, to prepare methanol-treated SF nanofiber matrices. The treatment time was varied from 2 to 120 min. The SF nanofiber matrices were placed in a desiccator saturated with water vapor and then dried in a vacuum at room temperature for 24 h to prepare the samples treated with water vapor. The treatment time was varied from 5 min to 6 h.

Weight Loss of Silk Fibroin Nanofiber in Water

Non-treated, methanol-treated, or water vapor-treated SF nanofiber matrices were immersed in distilled water and incubated at 25 °C for 30 min, followed by drying in a vacuum. Changes of the weight loss were measured and normalized to their initial values before immersion in water ($n = 3$).

Viscosity Measurements

The viscosity of the SF solutions was measured at 25 °C using an LVDVE 230 viscometer (Brookfield) equipped with a SC4-31 spindle and a 13R chamber (shear rate, 66 s^{-1}; sample volume, 16 mL; $n = 3$).

Spectroscopic Analysis

IR spectra of SF nanofiber matrices were taken using a Magma 560 spectrometer (Nicolet) at a resolution of 2 cm^{-1}. A custom-made chamber was used for the time-resolved measurements of the IR spectra of the water vapor-treated samples. The measurement was started once the water was placed in the chamber. The temperature was varied from 25 to 55 °C, and temperature control was achieved within ±0.1 °C. ^{13}C solid-state cross polarization, magic-angle spinning (CP/MAS) NMR spectra of the SF nanofibers were obtained on a DSX 400 NMR spectrometer (Bruker), using a cross-polarization pulse sequence and magic-angle spinning at 6.5 kHz. All of the spectra obtained by IR and NMR spectroscopy were separated into their separate components by a deconvolution method using a Gaussian function, in order to make quantitative analyses.

Morphology Analysis

A scanning electron microscope (Hitachi S-2350) was used to investigate the morphology of gold-coated SF nanofibers before and after the chemical treatments.

Mechanical Testing

The mechanical properties of the electrospun SF nanofiber matrices were measured using an Instron tensile tester. Samples were prepared according to the D-638-5 ASTM method and tested at 25 °C and 50% humidity ($n = 10$).

Cell Culture

Normal human epidermal keratinocytes (NHEK) were prepared and maintained, as previously reported.[19] Briefly,

NHEK were isolated from the foreskins of human subjects undergoing surgery. The epidermal keratinocytes were isolated from separated epithelial tissue by trypsinization, and primary cultures were established in a keratinocyte growth medium containing 0.15×10^{-3} M calcium and a supplementary growth factor bullet kit (KGM, Clonetics). Primary NHEK were cultured until the cells reached 70% confluence, and the second passage keratinocytes were used for this study. Primary normal human epidermal fibroblasts (NHEF) were also prepared and maintained as previously reported.[19] These tissue samples were also obtained from the foreskins of human subjects undergoing surgery. The samples were thoroughly washed with calcium- and magnesium-free Hanks' balanced salt solution (Invitrogen). Primary NHEF were established from explant cultures of foreskin, and they were serially subcultured and passaged at each 80% confluence level. The fourth passage fibroblasts were used for this study, and the cells were cultured in Dulbecco's modified Eagle's medium (DMEM; Sigma) supplemented with 10% fetal bovine serum. All procedures of sampling human tissue specimens were in accordance with guidelines of the Institutional Review Board (IRB) on Human Subjects Research and the Ethics Committee at the Seoul National University Dental Hospital, Seoul, Korea.

Cell Adhesion and Spreading

Cell adhesion was investigated using a modified method of Mould et al.[24] Regenerated SF nanofiber matrices were cut out with a punch (14 mm diameter) and placed in 24-well tissue culture plates. The plates containing the SF nanofiber matrices were first treated with PBS containing 0.1% heat-inactivated bovine serum albumin (BSA, Sigma) for 1 h at room temperature. The plates were then rinsed with fresh PBS. The cells were resuspended in the culture media (1×10^5 cells per 500 μL), added to each plate, and incubated for 1 h at 37 °C. Non-adhered cells were removed by two rinses with PBS. Adhered cells were fixed with 10% formalin in PBS for 15 min, rinsed twice with PBS, and stained with hematoxylin and eosin. To ensure a representative count, each sample was divided into quarters, and two fields per quarter were photographed with an Olympus BX51 microscope at 100×.

Cell spreading was studied by image analysis of NHEK and NHEF adhered onto the SF nanofiber matrices. Only the cells that adopted a flattened, polygonal shape with filopodia- and lamellipodia-like extensions were regarded as spreading cells. The percentage of cells that displayed a spreading morphology was quantified and normalized by the total number of adhered cells.

Statistical Analysis

The adhesion and spreading of cells onto polystyrene tissue culture plates, and onto water vapor- and methanol-treated SF nanofiber matrices were compared using the STATISTICA 6.0 software package. Unpaired student *t*-tests were performed for two-tailed *P*-value determination. Differences were considered statistically significant when the *P*-values were less than 0.05.

Results and Discussion

Characteristics of Electrospun Silk Fibroin Nanofibers

Regenerated silk fibroin (SF) was dissolved in HFIP, and its viscosity was measured at various concentrations as shown in Figure 1. The viscosity of the SF solution began to increase significantly at a concentration of 7%, due to the entanglement of the SF macromolecular chains. Non-woven matrices composed of randomly-arranged nanofibers were prepared by electrospinning the SF solution at this concentration. The mean diameter of the electrospun nanofibers was 380 nm with a unimodal size distribution in the range of 250–530 nm, which was determined by image analysis of scanning electron microscopic pictures (Figure 2).

Weight Loss of Silk Fibroin Nanofiber Matrices After Treatment

Non-treated SF nanofiber matrices are easily swollen and are readily soluble in water unless stabilized by treatment with certain organic solvents. The SF nanofiber matrices were treated either with an aqueous methanol solution or with water vapor to enhance the stability of the nanofiber matrices in water. An aqueous methanol solution is one of the commonly used organic solvents for this purpose, and the weight loss of the SF nanofiber matrices instantly decreased after they were treated with an aqueous methanol solution (Figure 3A). However, the methanol-treated SF matrices typically have a high content of crystalline regions, and are often very brittle. The mechanical properties of the SF nanofiber matrices are strongly dependent on the crystalline structures of the nanofibers. Various mechanical properties of SF nanofiber matrices, treated with either water vapor or a methanol solution, are listed and compared with those of non-treated nanofiber matrices in Table 1. The tensile modulus of the methanol-treated SF

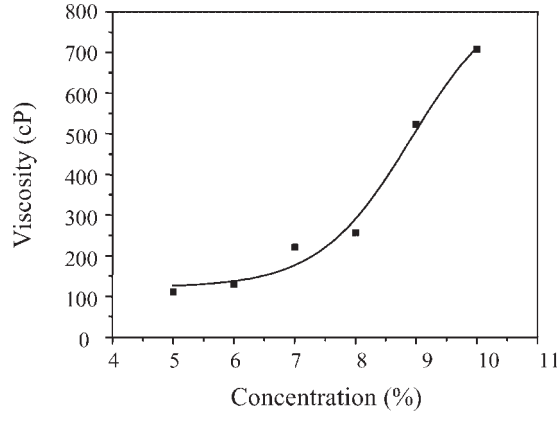

Figure 1. Viscosity plotted against concentration for regenerated silk fibroin dissolved in hexafluoro-2-propanol (HFIP).

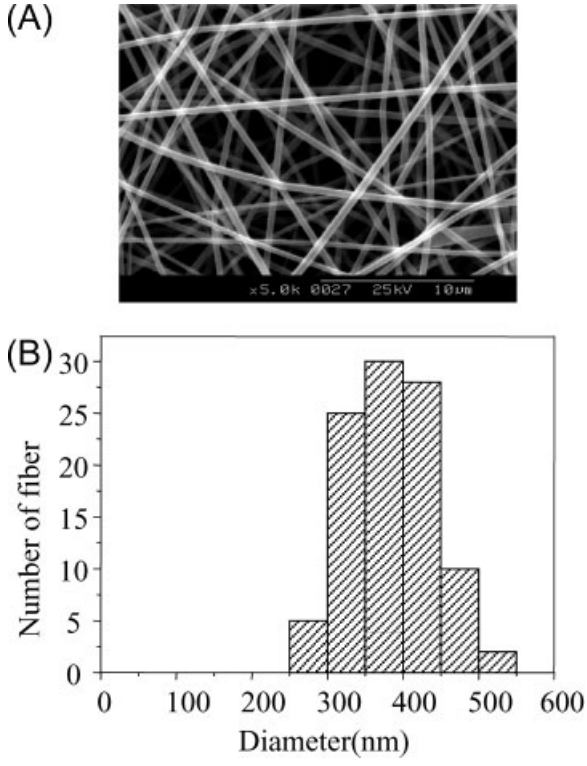

Figure 2. (A) Scanning electron microscopic picture and (B) fiber diameter distribution of electrospun SF nanofibers.

nanofiber matrices was substantially increased, compared to non-treated nanofiber matrices, due to the increment of the crystalline regions of the fibroin nanofibers. In contrast, the elongation at break of the methanol-treated samples decreased, indicating a hard and brittle nanofiber matrix formation, which may not be useful for wound dressings, nor for cell culturing onto matrices for practical tissue engineering applications. Although the yield stress of the water vapor-treated nanofiber matrices increased, the elongation at break was not significantly changed, compared with the non-treated SF nanofiber matrices, indicating a stronger matrix formation than the untreated matrices, but less brittle than the methanol-treated ones.

It was reported that annealing of regenerated SF films in water at room temperature was effective at inducing the formation of crystalline structures with less brittle characteristics.[22] However, this method was only effective for films >70 μm thick, and the SF nanofiber matrices in our study were treated with water vapor instead of water. The weight loss of the SF nanofiber matrices treated with water vapor was about 15%, which was quite similar to that of matrices treated with an aqueous methanol solution. Non-treated SF nanofiber matrices lost about 35% of their own weight in water. The water vapor treatment method at low temperature required a longer treatment time rather than the methanol-treatment method (Figure 3B). However, the stabilization of the SF nanofiber matrix was completed within 10 min, as the water vapor treatment temperature increased from 25 to 55 °C. The constant weight loss of the nanofiber matrices treated either with water vapor or with methanol for longer time periods could be attributed to the remaining HFIP in the matrices. The morphology of the methanol-treated SF nanofiber matrices was significantly changed. This was probably due to the swelling of the SF nanofibers by water during treatment (Figure 4C). Although the methanol-treated SF nanofiber matrices showed enhanced mechanical properties compared with those of non-treated SF nanofiber matrices, the loss of the porous structures in the matrices could limit their use in certain biomedical applications, including tissue engineering.

Structural Changes of Silk Fibroin Nanofibers During Treatment

The major conformations of SF are random coil, α-helix, and β-sheet.[5] The crystallization of SF can be easily induced by simple physical (e.g., thermal)[25] or chemical (e.g., methanol)[26] treatments. The most common method of converting a random coil form of SF into a more stable β-sheet conformation is treatment of the matrices with an organic solvent. It is well accepted that using a methanol treatment is highly effective in the crystallization of SF from a random coil conformation to a β-sheet conformation.

The infrared (IR) spectroscopic method has been frequently used to investigate the conformational changes of silk fibroin.[27–29] The characteristic absorption bands of SF are found in the regions of 1 625 cm^{-1} (amide I), 1 528 cm^{-1} (amide II), 1 230 cm^{-1} (amide III), and 700 cm^{-1} (amide V). The characteristic absorption bands of non-treated SF nanofibers were observed at 1 647 cm^{-1} (amide I) and 1 541 cm^{-1} (amide II), which can be attributed to the random coil conformation (Figure 5A). Interestingly, these bands were shifted to 1 624 cm^{-1} (amide I) and 1 519 cm^{-1} (amide II) during the water vapor treatment, which is indicative of structural changes in the SF, from a random coil conformation to a β-sheet conformation. It was hypothesized that the SF macromolecules could rearrange to change the crystal structures due to the changes in the hydrogen bonding caused by the water vapor. SF nanofiber matrices treated with an aqueous methanol solution showed characteristic absorption bands at 1 620 cm^{-1} (amide I) and 1 516 cm^{-1} (amide II), which are strongly related to the β-sheet conformation.

Time-resolved measurements of IR absorption bands provided a useful means of monitoring the structural changes of the macromolecules as a function of treatment time.[30] Changes in the characteristic absorption peaks of the amide I and II bands of the SF nanofibers during the water vapor treatment at 35 °C are shown in Figure 5B. The peak position of the SF nanofibers treated with water vapor at 35 °C reached 1 627 cm^{-1} in approximately 30 min, and it approached 1 623 cm^{-1} in 10 min at 55 °C (data not shown),

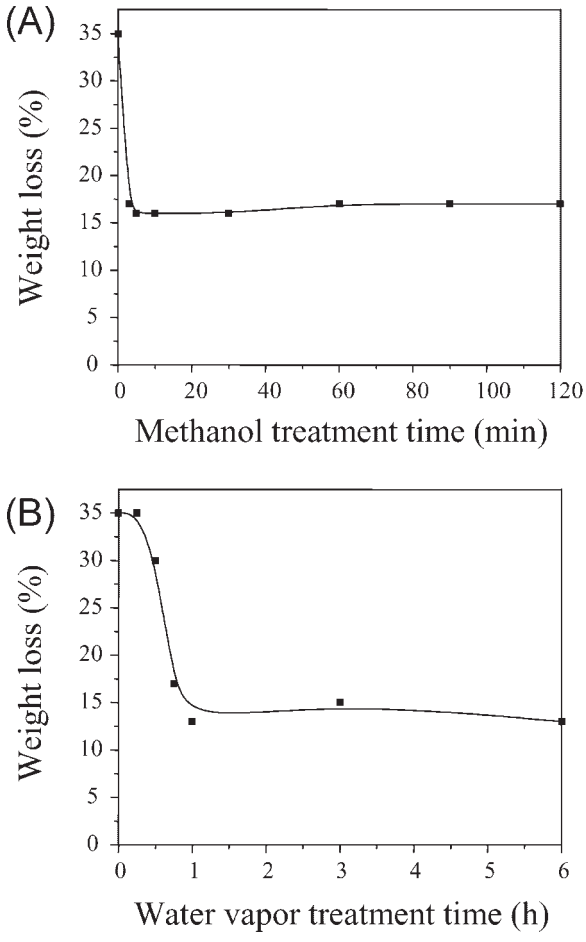

Figure 3. Weight loss of electrospun SF nanofibers treated with (A) an aqueous methanol solution and (B) water vapor as a function of treatment time at 25 °C.

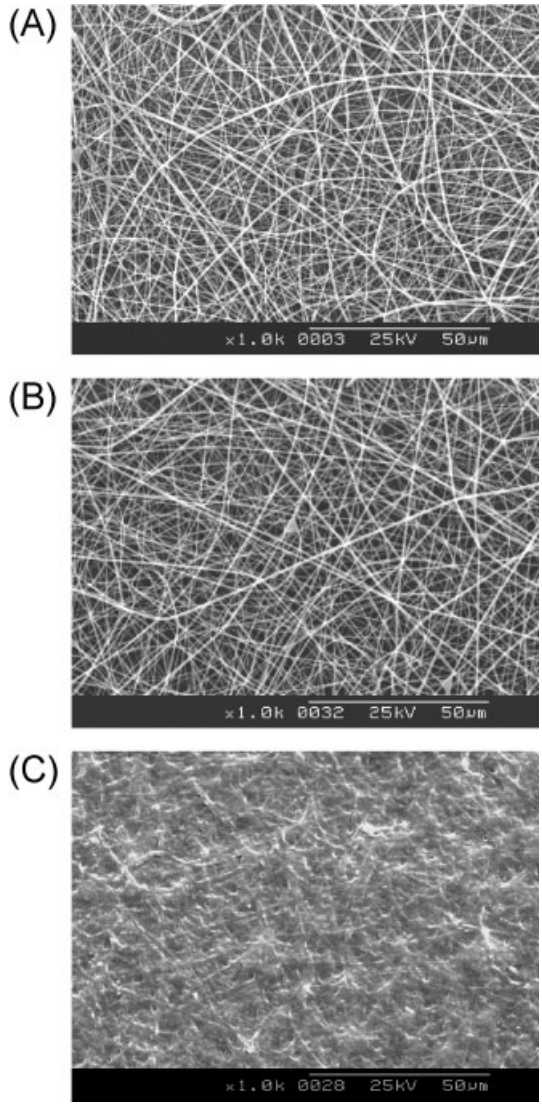

Figure 4. Scanning electron microscopic pictures of (A) non-treated, (B) water vapor-treated, and (C) methanol-treated SF nanofibers.

which was quite similar to the response of SF nanofibers treated with an aqueous methanol solution at 25 °C. The shift rate of the peak position of the amide I band increased as the temperature increased. Changes in the ratio of the peak areas of β-sheet and random coil structures (A_{II}/A_I) in the amide II region were determined from the IR spectra during the water vapor treatment. The temperature at which the SF nanofiber matrices were treated was a critical factor in controlling the crystallization kinetics, and the structural changes from the random coil conformation to the β-sheet conformation of the SF nanofiber matrices treated with water vapor were complete in 10 min at above 45 °C (Figure 6). Changes in the ratio of peak areas (A_{II}/A_I) in the amide I region were similar to those observed in the amide II region (data not shown).

Table 1. Mechanical properties of regenerated silk fibroin nanofiber matrices.

Samples	Yield stress	Elongation at break	Tensile modulus
	MPa	%	MPa
Non-treated	1.3 ± 0.2	7.6 ± 1.7	17.7 ± 6.8
Water vapor-treated	2.6 ± 0.4	8.5 ± 2.0	30.4 ± 4.4
Methanol-treated	4.6 ± 0.5	4.4 ± 0.7	104.3 ± 13.7

Solid-state ^{13}C NMR spectroscopy also provides a powerful means of confirming the structural changes of the silk proteins from the random coil conformation to the β-sheet conformation, as the chemical shifts of the carbon atoms in silk proteins are strongly related to the secondary structure of the β-sheet conformations. The β-sheet form can be identified by the ^{13}C chemical shifts of Gly (glycine), Ser (serine), and Ala (alanine) that are indicative of β-sheet conformations.[31] Ala is a major constituent of SF,[32] and the chemical shifts of Ala, particularly of the methyl groups

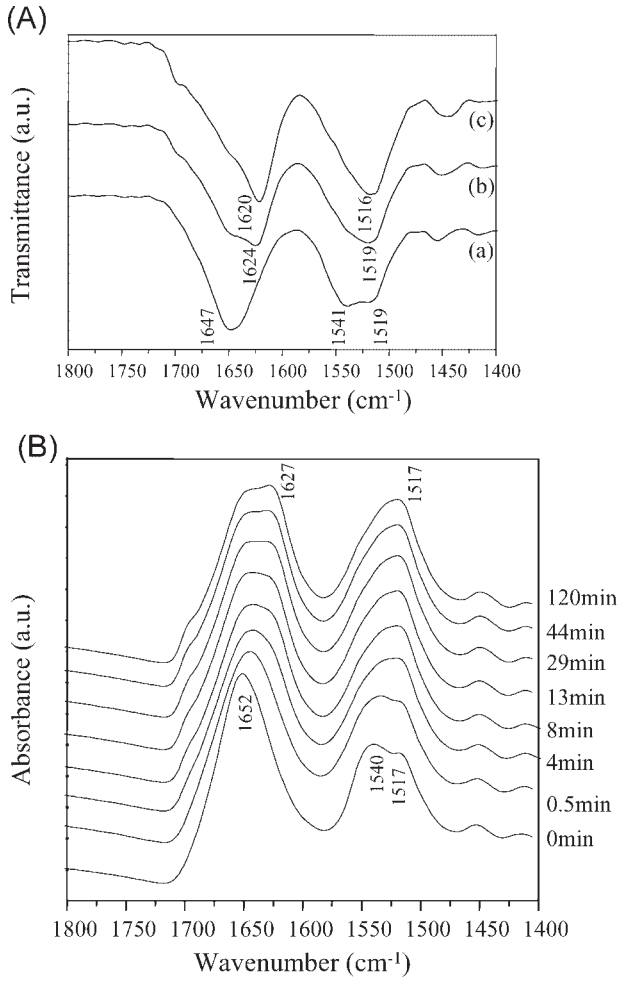

Figure 5. (A) IR spectra of (a) non-treated, (b) water vapor-treated, and (c) methanol-treated silk fibroin nanofibers. (B) Time-dependent changes in the IR spectra of regenerated SF nanofibers treated with water vapor at 35 °C.

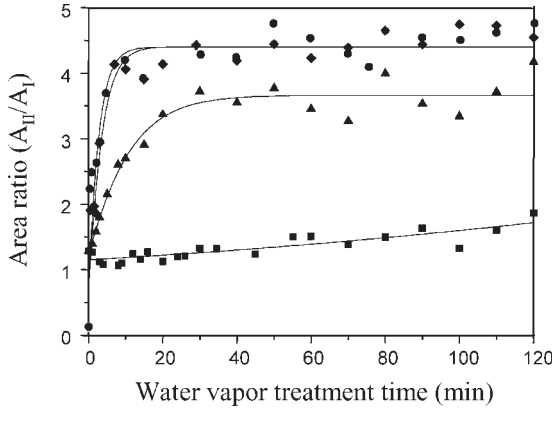

Figure 6. Changes in the area ratios of β-sheet and random coil structures (A_{II}/A_I) in the amide II region of the SF nanofibers, as determined from IR spectra during water vapor treatment at various temperatures (■, 25 °C; ▲, 35 °C; ◆, 45 °C; ●, 55 °C).

of the Ala residues (Ala C_β), are representative of the conformational status of the protein (Figure 7A). Expanded views of the chemical shifts of the Ala C_β region in the SF nanofibers are shown in Figure 7B. The chemical shift of Ala C_β in non-treated SF nanofibers was 16.3 ppm, indicating that the Ala residues of the SF nanofibers were mainly in the random coil conformation. The water vapor-treated SF nanofibers, however, showed a shoulder at 20.4 ppm, which can be assigned to Ala C_β in the β-sheet conformation. The shift of Ala C_β in the non-treated SF nanofibers was observed during water vapor treatment. The dotted line in Figure 7B indicates the curve-fitting results used to calculate the content of Ala residues found in the β-sheet conformation. The percentage expressed for each spectrum, which is the content of Ala residues contributing to the β-sheet structure formation, increased by treatment with both water vapor and methanol. This finding clearly indicates that the Ala residues in the SF nanofiber chains take the β-sheet conformation following water vapor treatment in a manner similar to those in methanol-treated

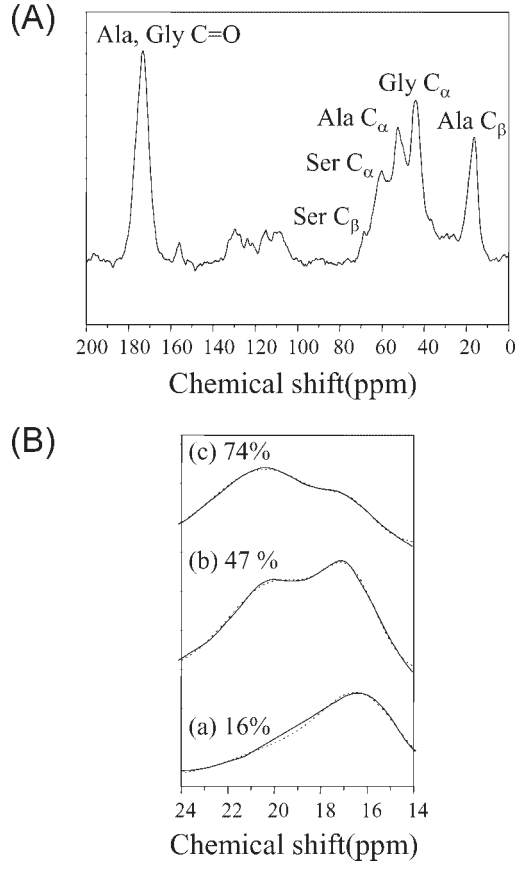

Figure 7. (A) ^{13}C NMR spectra of non-treated SF nanofibers. (B) Expanded ^{13}C NMR spectra of the alanine methyl region of (a) non-treated, (b) water vapor-treated, and (c) methanol-treated regenerated SF nanofibers. The dotted line indicates the curve-fitting result used to calculate the content of alanine residues found in the β-sheet conformation, as denoted by the percentages given for each spectrum.

fibroin chains. The β-sheet content of water-vapor-treated SF nanofibers (47%) was much lower than that of methanol-treated ones (74%)

Cell Adhesion and Spreading

Scaffolding materials for tissue engineering approaches are typically designed to promote cell growth and physiological functions, and to maintain normal states of cell differentiation.[33] *In vivo* implantation experiments of fibroin-coated polyester sutures have demonstrated that regenerated SF did not induce any significant thrombogenic responses.[11] In addition the low inflammatory potential of SF had already been reported.[13] Cellular responses to SF nanofiber matrices were investigated using normal human keratinocytes and fibroblasts *in vitro*, aimed at regenerating skin tissues via tissue engineering approaches. Since initial cell attachment and spreading could be important factors in developing wound dressings and scaffolds for tissue engineering, the initial cell attachment and spreading onto SF nanofiber matrices were first studied. In the case of biomedical applications, including guided tissue regeneration and burn wound dressings, the matrices that cover the wounds are usually in contact with blood proteins. Therefore, to assess cell attachment and spreading, cells were seeded onto SF nanofiber matrices after the matrices were treated with BSA. Photomicrographs of exponentially-proliferating NHEK and NHEF, adherent to the SF nanofiber matrices, were taken and used for the adhesion assay.

Figure 8A shows representative pictures of cells adhered to the SF nanofiber matrices. A relatively high number of NHEK were adherent to the SF nanofiber matrices, and there was no distinct difference in the number of cells adhered to the water vapor-treated and methanol-treated SF nanofiber matrices. In contrast, a relatively small number of NHEF adhered to the matrices, and the adhesion activity profile on the water vapor-treated SF nanofiber matrices was significantly higher than that on the methanol-treated SF nanofiber matrices (Figure 8B). We further investigated whether the adhered cells were only tethered to the substrate (non-spreading) or spread over the substrate (spreading). Photographs of NHEK and NHEF, adherent to SF nanofiber matrices, were taken and used for spreading assays (data not shown). Interestingly, the adhesion and spreading of cells adhered to both water vapor-treated and methanol-treated SF nanofiber matrices with a BSA coating showed similar trends. In the case of NHEK, a relatively high cell spreading profile was observed for both the water vapor-treated and methanol-treated SF nanofiber matrices. In contrast, the spreading of NHEF was significantly reduced as compared with that of NHEK. The percentage of cell spreading of NHEF on the water vapor-treated SF nanofiber matrices was, however, significantly higher than that on the methanol-treated SF nanofiber matrices (Figure 8C).

It is generally accepted that diverse cellular responses to synthetic surfaces arise from differences in the adsorption of extracellular matrix (ECM) proteins to surfaces. Different classes of cell adhesion receptors mediate interactions between cells and neighboring cells and the surrounding ECM. Among these receptors, integrins primarily mediate the interactions between cells and ECM components, and transmit biochemical signals across the plasma membrane. It is well known that integrins expressed on cell surfaces differ among cells or cell types, and that three major integrins, such as $\alpha_2\beta_1$, $\alpha_3\beta_1$, and $\alpha_6\beta_4$ are expressed in the normal basal keratinocyte layer.[34] Our previous reports

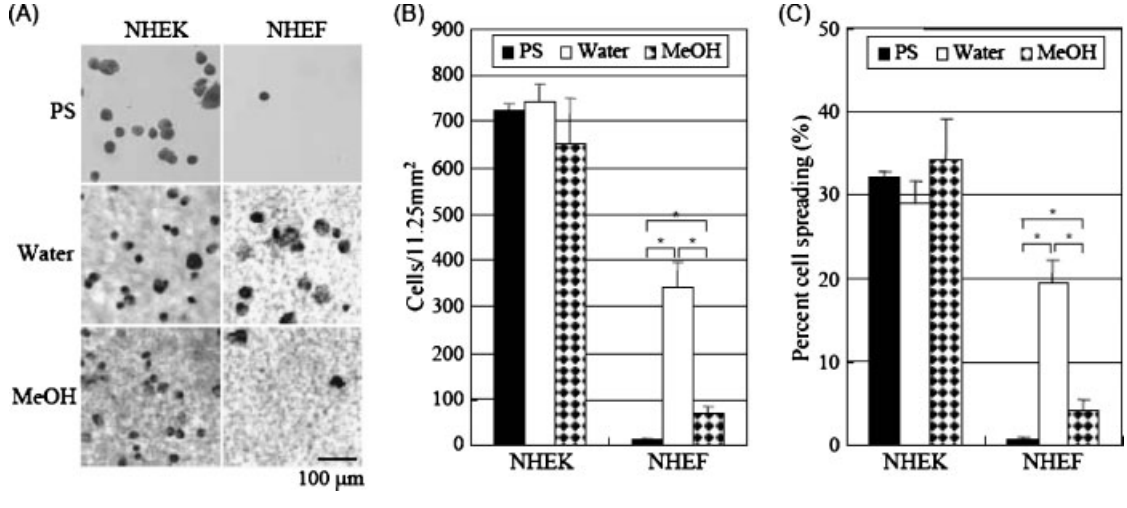

Figure 8. (A) Photographs and (B) the numbers of NHEK and NHEF adhered to water vapor-treated and methanol-treated SF nanofibers. (C) Percentage of cell spreading for NHEK and NHEF plated onto water vapor-treated and methanol-treated SF nanofibers. Data are expressed as mean $\pm$ standard deviation ($n = 4$). An asterisk indicates a statistically significant difference ($P < 0.05$). PS: polystyrene tissue culture plate; Water: water vapor-treated SF nanofibers; MeOH: methanol-treated SF nanofibers.

have also shown that expression levels of integrin subunits in normal human fibroblasts were much different to those of normal human keratinocytes.[35,36] Furthermore, cellular attachment is known to be regulated by selective expression of integrins[37,38] and by modulation of the binding properties of the integrin receptors.[39,40] It is unclear why only the adhesion and spreading of fibroblasts adhered to SF nanofiber matrices was improved by water vapor treatment, unlike keratinocytes. However, it could be attributed to different cell types with different types of integrin.

Conclusion

The secondary structure of the regenerated SF nanofibers was greatly altered by treatment, either with methanol or with water vapor via solvent-induced conformational transitions, which were confirmed by time-resolved IR and solid-state ^{13}C CP-MAS NMR spectroscopy. Water vapor treatment was useful for inducing the conformational changes of SF nanofibers from a random coil form to a β-sheet form, and these structural changes were strongly dependent on the treatment time and temperature. In the cytocompatibility assessment, water vapor-treated SF nanofiber matrices were found to be promising scaffolds for the adhesion and spreading of normal human keratinocytes and fibroblasts, as compared to methanol-treated SF nanofiber matrices. This approach to controlling the structures of regenerated SF nanofibers may be useful in designing and fabricating regenerated SF matrices for wound dressings and tissue engineering applications.

Acknowledgements: This work was supported by the *NanoBio R&D Program* (Grant No. 2005-00009 and 2005-00115) of the *Korea Science & Engineering Foundation*.

[1] D. Kaplan, W. W. Adams, B. Farmer, C. Viney, "*Silk – Biology, Structure, Properties, and Genetics*", ACS Symposium Series 544, Washington, DC 1994.
[2] M. Li, S. Lu, Z. Wu, K. Tan, N. Minoura, S. Kuga, *Int. J. Biol. Macromol.* **2002**, *30*, 89.
[3] J. Yao, H. Masuda, C. Zhao, T. Asakura, *Macromolecules* **2002**, *35*, 6.
[4] S. Putthanarat, S. Zarkoob, J. Magoshi, J. A. Che, R. K. Eby, M. Stone, W. W. Adams, *Polymer* **2002**, *43*, 3405.
[5] J. Ayutsede, M. Gandhi, S. Sukigara, M. Micklus, H. E. Chen, F. Ko, *Polymer* **2005**, *46*, 1625.
[6] H. J. Jin, D. L. Kaplan, *Nature* **2003**, *424*, 1057.
[7] M. N. Padamwar, A. P. Pawar, *J. Sci. Ind. Res.* **2004**, *63*, 323.
[8] K. Fuji, S. Takahashi, R. Kinouchi, *Jpn. Soc. Food Sci. Technol.* **2000**, *47*, 363.
[9] A. Motta, C. Migliaresi, F. Faccioni, P. Torricelli, M. Fini, R. Giardino, *J. Biomater. Sci., Polym. Ed.* **2004**, *15*, 851.
[10] A. Motta, C. Migliaresi, A. W. Lloyd, S. P. Denyer, M. Santin, *J. Bioact. Compat. Polym.* **2002**, *17*, 23.
[11] H. Sakabe, H. Ito, T. Miyamoto, Y. Noishiki, W. S. Ha, *Sen'i Gakkaishi* **1989**, *45*, 487.
[12] W. H. Park, W. S. Ha, H. Ito, T. Miyamoto, H. Inagaki, Y. Noishiki, *Fibers Polym.* **2001**, *2*, 58.
[13] M. Santi, A. Motta, G. Freddi, M. Cannas, *J. Biomed. Mater. Res.* **1999**, *46*, 382.
[14] K. Cai, K. Yao, Y. Cui, Z. Yang, X. Li, H. Xie, T. Qing, L. Gao, *Biomaterials* **2002**, *23*, 1603.
[15] K. Cai, K. Yao, S. Lin, Z. Yang, X. Li, H. Xie, T. Qing, L. Gao, *Biomaterials* **2002**, *23*, 1153.
[16] B. M. Min, L. Jeong, Y. S. Nam, J. M. Kim, J. Y. Kim, W. H. Park, *Int. J. Biol. Macromol.* **2004**, *34*, 281.
[17] V. Karageorgiou, L. Meinel, S. Hofmann, A. Malhotra, V. Volloch, D. Kaplan, *J. Biomed. Mater. Res.* **2004**, *71A*, 528.
[18] S. H. Kim, Y. S. Nam, T. S. Lee, W. H. Park, *Polym. J.* **2003**, *35*, 185.
[19] B. M. Min, G. Lee, S. H. Kim, Y. S. Nam, T. S. Lee, W. H. Park, *Biomaterials* **2004**, *25*, 1289.
[20] M. Ishida, T. Asakura, M. Yokoi, H. Saito, *Macromolecules* **1990**, *23*, 88.
[21] M. Tsukada, Y. Gotoh, M. Nagura, N. Minoura, N. Kasai, G. Freddi, *J. Polym. Sci., Part B: Polym. Phys.* **1994**, *32*, 961.
[22] H. J. Jin, J. Park, V. Karageorgiou, U. J. Kim, R. Valluzzi, P. Cebe, D. L. Kaplan, *Adv. Funct. Mater.* **2005**, *15*, 1241.
[23] T. Asakura, M. Demura, Y. Watanabe, K. Sato, *J. Polym. Sci., Part B: Polym. Phys.* **1992**, *30*, 693.
[24] A. P. Mould, J. A. Askari, M. J. Humphries, *J. Biol. Chem.* **2000**, *275*, 20324.
[25] X. N. Peng, X. Chen, P. Y. Wu, Z. Z. Shao, *Acta Chim. Sin.* **2004**, *62*, 2127.
[26] D. Wilson, R. Valluzzi, D. Kaplan, *Biophysical J.* **2000**, *78*, 2690.
[27] M. Tsukada, G. Freddi, P. Monti, N. Kasai, *J. Polym. Sci., Part B: Polym. Phys.* **1995**, *33*, 1995.
[28] X. Chen, D. P. Knight, Z. Shao, F. Vollrath, *Polymer* **2001**, *42*, 9969.
[29] A. B. Mathur, A. Tonelli, T. Rathke, S. Hudson, *Biopolymers* **1997**, *42*, 61.
[30] X. Chen, D. P. Knight, Z. Z. Shao, F. Vollrath, *Biochemistry* **2002**, *41*, 14944.
[31] T. Asakura, J. Yao, T. Yamane, K. Umemura, A. S. Ulrich, *J. Am. Chem. Soc.* **2002**, *124*, 8794.
[32] H. Saito, R. Tabeta, T. Asakura, Y. Iwanaga, A. Shoji, T. Ozaki, I. Ando, *Macromolecules* **1984**, *17*, 1405.
[33] M. P. Lutolf, J. A. Hubbell, *Nat. Biotechnol.* **2005**, *23*, 47.
[34] J. C. Adams, F. M. Watt, *Development* **1993**, *117*, 1183.
[35] B. S. Park, S. J. Heo, C. S. Kim, J. E. Oh, J. M. Kim, G. Lee, W. H. Park, C. P. Chung, B. M. Min, *J. Biomed. Mater. Res.* **2005**, *74A*, 640.
[36] J. E. Oh, K. H. Park, H. K. Noh, J. M. Kim, C. P. Chung, B. M. Min, *Cell Commun. Adhes.* **2002**, *9*, 173.
[37] M. Guo, L. T. Kim, S. K. Akiyama, H. R. Gralnick, K. M. Yamada, F. Grinnell, *Exp. Cell Res.* **1991**, *195*, 315.
[38] J. P. Kim, K. Zhang, J. D. Chen, K. C. Wynn, R. H. Kramer, D. T. Woodley, *J. Cell Physiol.* **1992**, *151*, 443.
[39] P. Sánchez-Mateos, C. Cabanas, F. Sánchez-Madrid, *Semin. Cancer Biol.* **1996**, *7*, 99.
[40] M. A. Schwartz, M. D. Schaller, M. H. Ginsberg, *Ann. Rev. Cell Dev. Biol.* **1995**, *11*, 549.

